Multichannel Random Discrete Fractional Fourier Transform

Xuejing Kang, Feng Zhang, *Member, IEEE*, and Ran Tao, *Senior Member, IEEE*

***Abstract*—We propose a multichannel random discrete fractional Fourier transform (MRFrFT) with random weighting coefficients and partial transform kernel functions. First, the weighting coefficients of each channel are randomized. Then, the kernel functions, selected based on a choice scheme, are randomized using a group of random phase-only masks (RPOMs). The proposed MRFrFT can be carried out both electronically and optically, and its main features and properties have been given. Numerical simulation about one-dimensional signal demonstrates that the MRFrFT has an important feature that the magnitude and phase of its output are both random. Moreover, the MRFrFT of two-dimensional image can be viewed as a security enhanced image encryption scheme due to the large key space and the sensitivity to the private keys.**

***Index Terms*—Chaotic logistic map, fractional Fourier transform, image encryption, random phase mask.**

I. Introduction

In THE past decades, the fractional Fourier transform (FrFT) has been regarded as a powerful tool in the fields of signal processing [1]–[4] and image processing [5]–[8]. An effective eigen-decomposition-based definition of discrete fractional Fourier transform (DFrFT) has been proposed by Pei [9], which can be viewed as the approximate samples of the continuous FrFT [1]. Some researchers have thoroughly studied this definition and found that changing its eigenvalue or eigenvector will create totally different transforms with new properties and applications. Based on this idea, fruitful expansions of the FrFT, for instance, the multiple-parameter discrete fractional Fourier transform (MPDFrFT) [10], the discrete fractional random transform (DFrNT) [11], and the random discrete fractional Fourier transform (RDFrFT) [12], have been presented. However, these expansions spend much time when implementing them on a computer because their kernel functions need to be recomputed once the transform order is changed [13]. Unlike the FrFT, these expansions cannot be implemented exactly in optics equipment because of the difficulties of randomizing the eigenfunctions and eigenvalues in optical system [14], [15]. To implementing the random FrFT in optics, Liu [14] presented a random fractional Fourier transform (RFrFT) by randomizing the kernel function of the continue FrFT using a couple mutually conjugated pure phase masks. But it also suffers the same time-consuming problem as other FrFT expansions and its key space is small when directly using it in image encryption and decryption.

In this letter, we propose an efficient multichannel random discrete fractional Fourier transform (MRFrFT) which is completed by three steps. First, the weighting coefficients of each channel are randomized. Then, the partial kernel functions, chosen by a choice mechanism that is completed based on the logistic map [8], are randomized by a group of random phase-only masks (RPOMs). The proposed MRFrFT can be carried out on a computer rapidly with an advantage that its kernel functions can be pre-computed and stored. Also it can be implemented by optoelectronic equipment. The main features and properties of the MRFrFT have been presented. Numerical simulation about one-dimensional (1D) signal verifies that the proposed MRFrFT has an important feature that the magnitude and phase of its output are both random. Moreover, the MRFrFT of two-dimensional (2D) image can be viewed as a security enhanced image encryption scheme due to the large key space and the sensitivity to the private keys.

II. Preliminaries

The ath-order $N \times N$ DFrFT $\mathbf{F}^a$ defined in [9] is:

$$\mathbf{F}^a = \mathbf{V}\mathbf{D}^a\mathbf{V}^T = \sum_{k=0}^{N-1} \exp\left[-j\left(\pi/2\right)ak\right]\mathbf{v}_k\mathbf{v}_k^T \tag{1}$$

where $\mathbf{v}_k$ is the kth-order discrete Fourier transform (DFT) Hermite-Gauss eigenvector, and $\mathbf{V} = [\mathbf{v}_0|\mathbf{v}_1|\cdots|\mathbf{v}_{N-2}|\mathbf{v}_{N-1}]$ for N is odd, $\mathbf{V} = [\mathbf{v}_0|\mathbf{v}_1|\cdots|\mathbf{v}_{N-2}|\mathbf{v}_N]$ for N is even. $\mathbf{D}^a$ is a diagonal matrix with diagonal entries corresponding to the eigenvalues for column eigenvectors in matrix $\mathbf{V}$, T denotes the matrix transpose.

Based on this definition, Yeh and Pei [13] developed a fast computation method for the DFrFT. Assume $\mathbf{x}$ be a N-point discrete signal, the ath-order DFrFT of the signal $\mathbf{x}$ is

$$\begin{cases} \mathbf{X}_a &= \sum_{n=0}^{N-1} B_{n,a}\mathbf{X}_{nb} \quad N \text{ odd} \\ \mathbf{X}_a &= \sum_{n=0}^{N} B_{n,a}\mathbf{X}_{nb} \quad N \text{ even} \end{cases} \tag{2}$$

where $b = 4/N$ for N is odd, $b = 4/(N+1)(N+1)$ for N is even, $\mathbf{X}_{nb}$ is the nbth-order DFrFT of signal $\mathbf{x}$. The weighting coefficients $B_{n,a}$ are computed as:

$$\begin{cases} B_{n,a} &= \mathrm{IDFT}\{\exp\left[-j\left(\pi/2\right)ak\right]\}_{k=0,1,2,\cdots,N-1} \quad N \text{ odd} \\ B_{n,a} &= \mathrm{IDFT}\{\exp\left[-j\left(\pi/2\right)ak\right]\}_{k=0,1,2,\cdots,N} \quad N \text{ even} \end{cases} \tag{3}$$

where IDFT$\{\cdot\}$ denotes a reverse DFT (*Proof:* see [13]).

From (2), the ath-order DFrFT $\mathbf{X}_a$ can be computed by a linear combination of N channels DFrFT $\mathbf{X}_{nb}$. Since N odd and even are essentially the same, we only consider the odd case for simplicity in the following.

Manuscript received January 07, 2015; accepted February 07, 2015. Date of publication February 10, 2015; date of current version February 20, 2015. This work was supported in part by the National Natural Science Foundation of China under Grants 61201354, 61331021, and 61421001, and by the Beijing Higher Education Young Elite Teacher Project under Grant YETP1221. The associate editor coordinating the review of this manuscript and approving it for publication was Prof. Yiannis Andreopoulos.

The authors are with the Department of Electronic Engineering, Beijing Institute of Technology, Beijing 100081, China, and also with Beijing Key Laboratory of Fractional Signals and Systems, Beijing 100081, China (e-mail: oUo@bit.edu.cn;kangxuejing@bit.edu.cn; rantao@bit.edu.cn).

(*Corresponding author: F. Zhang*.)

Color versions of one or more of the figures in this paper are available online at http://ieeexplore.ieee.org.

Digital Object Identifier 10.1109/LSP.2015.2402395

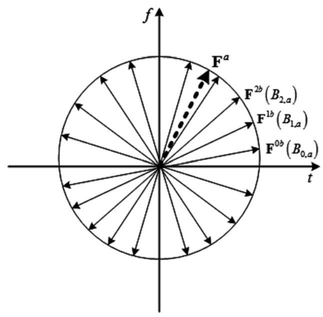

Fig. 1. Time-frequency denotation of $\mathbf{F}^{nb}$ and $\mathbf{F}^{a}$.

III. Multichannel Random Discrete Fractional Fourier Transform

A. The Proposed MRFrFT

Inspired by the computation method of the DFrFT presented in [13], we propose the MRFrFT by implementing the following three steps.

Step 1. Randomize the weighting coefficients.

From (1) and (3), the ath-order $N \times N$ DFrFT matrix can be computed by

$$\begin{aligned}\mathbf{F}^{a} &= \sum\nolimits_{k=0}^{N-1} \exp\left[-j\left(\pi/2\right)ak\right]\mathbf{v}_k\mathbf{v}_k^T \\ &= \sum\nolimits_{k=0}^{N-1} \left\{\sum\nolimits_{n=0}^{N-1} B_{n,a}\exp\left[-j\left(2\pi/N\right)nk\right]\right\}\mathbf{v}_k\mathbf{v}_k^T \\ &= \sum\nolimits_{n=0}^{N-1} B_{n,a}\left\{\sum\nolimits_{k=0}^{N-1} \exp\left[-j\left(2\pi/N\right)nk\right]\mathbf{v}_k\mathbf{v}_k^T\right\} \\ &= \sum_{n=0}^{N-1} B_{n,a}\mathbf{F}^{nb} \end{aligned} \tag{4}$$

where $b = 4/N$, $\mathbf{F}^{nb}$ are nbth-order $N \times N$ DFrFT matrices.

This implies that the DFrFT of any angle can be computed by a weighted summation of the DFrFTs with N special angles. It is well known that the interpretation of the FrFT is a rotation of signals in the time-frequency plane [16], [17]. Therefore the time-frequency denotation of $\mathbf{F}^{nb}$ and $\mathbf{F}^{a}$ can be illustrated by Fig. 1. In the parentheses are the corresponding channel weighting coefficients.

In (4), the eigenvalue of $\mathbf{F}^{a}$ is divided into the coefficients of every channel and the eigenvalues of matrices $\mathbf{F}^{nb}$. From [18], we have the conclusion that for each eigenfunction, the corresponding eigenvalue has infinite choices, which suggests that they can be chosen in an absolutely random way. Here, we randomize the coefficients of every channel as follows:

$$B_n^{R_n} = \mathrm{IDFT}\{\exp\left[-j\left(\pi/2\right)k\cdot\mathrm{Rand}\left(n\right)\right]\}_k \tag{5}$$

where $\mathrm{Rand}(n) \in [0,1]n = 0,1,\cdots,N-1$ are random numbers whose values are independent of n. The random coefficients vector is denoted as $\mathbf{B} = \{B_n^{R_n}, n = 0,1,\cdots,N-1\}$. ■

Step 2. Randomize the transform kernel function.

From (4), the nbth-channel kernel function with the eigendecomposition form is

$$\mathbf{F}^{nb} = \sum\nolimits_{k=0}^{N-1} \exp\left[-j\left(\pi/2\right)k\cdot nb\right]\mathbf{v}_k\mathbf{v}_k^T = \mathbf{V}\mathbf{\Lambda}_n\mathbf{V}^T \tag{6}$$

with $\mathbf{\Lambda}_n = \mathrm{diag}\{\exp[-j\frac{\pi}{2}nb\cdot 0],\cdots,\exp[-j\frac{\pi}{2}nb\cdot(N-1)]\}$. We randomize the kernel function $\mathbf{F}^{nb}$ as follows:

$$\mathbf{R}_n = \mathbf{P}_n^1\cdot\mathbf{F}^{nb}\cdot\mathbf{P}_n^2 \tag{7}$$

where $\mathbf{P}_n^i = \exp[-j2\pi P_n^i(v)], i = 1,2$ are two RPOMs used to confuse the corresponding kernel function $\mathbf{F}^{nb}$. $P_n^i(v), i = 1,2$ are two mutual independent white noise matrices and uniformly distributed in $[0;1]$. ■

Based on Step 1 and Step 2, the MRFrFT can be defined as

$$\mathbf{F}^{R} = \sum\nolimits_{n=0}^{N-1} B_n^{R_n}\mathbf{R}_n \tag{8}$$

It must be noted that in (8), N channels MRFrFT need to produce $2N$ RPOMs, which is time-consuming and sometimes unnecessary. This shortcoming motivates us to find a choice mechanism which can randomly select several channels kernel functions and then randomize them by (7). Step 3 gives a choice mechanism based on chaos mapping.

Step 3. A choice mechanism for selecting channels.

In this part, a choice mechanism based on pseudorandom address sequence generated by the logistic map is presented. The logistic map is a nonlinear chaos function and very sensitive to the initial parameters. Its iterative form is written as

$$x_{n+1} = p\cdot x_n\cdot(1-x_n) \tag{9}$$

where $0 \le p \le 4$, is a system parameter known as bifurcation parameter. $x_n \in (0,1)$ denotes the iterative value and x_0 is the initial value. When $p \in [3.5699456, 4]$, the dynamical system is in chaotic state. Slight variations of the initial parameter can yield a totally different random iterative value, which is a non-periodic and non-converging sequence over time.

Based on the feature of the logistic map, we use it to propose a choice scheme for selecting channels.

1) Giving the system parameter p and the initial value x_0, use (9) to generate a random sequence with length N. We will obtain a pseudorandom sequence $X = \{x(n)|n = 0,1,\cdots,N-1\}$.
2) Sorting X in ascending order, we will get a sorted sequence $X' = \{x[d(n)]|n = 0,1,\cdots,N-1\}$, where the symbol $d(n)$ denotes the address code. That is, the elements values are not changed but the positions are varied. For example, the n-th element in X' corresponds to the $d(n)$-th element in X.
3) Giving an integer K and discarding the pervious K value from the random sequences X', we will obtain $X' = \{x[d(m)]|m = 0,1,\cdots,N-1-K\}$.
4) A pseudorandom address sequence is generated as $\{d(m)|m = 0,1,\cdots,N-1-K\}$.
5) Select the $d(m)$-th channel kernel matrices $\mathbf{F}^{d(m)b}(m = 0,1,\cdots,N-1-K)$ and randomize them by (7). ■

Use $\mathbf{Rand}$ denotes the linear combination of the randomized channels generated by step 3. It can be computed as

$$\mathbf{Rand} = \sum\nolimits_{m=0}^{N-1-K} B_{d(m)}^{R_{d(m)}}\mathbf{R}_{d(m)} \tag{10}$$

Use $\mathbf{Fr}$ denotes the linear combination of the rest channels. It can be computed as

$$\mathbf{Fr} = \sum_{n} B_n^{R_n} \mathbf{F}^{nb} \tag{11}$$

where
$n \in \{n|\{0,1,\cdots,N-1\}\backslash\{d(m)|m=0,1,\cdots,N-1-K\}\}$.

Therefore, the proposed MRFrFT matrix (8) is adjusted as:

$$\mathbf{F}^{R} = \mathbf{Rand} + \mathbf{Fr} \tag{12}$$

Thus, the MRFrFT of a 1D discrete signal $\mathbf{x}$ is computed as:

$$\mathbf{X}_R = \mathbf{F}^R \mathbf{x} \tag{13}$$

The transform kernel of the 2D MRFrFT is defined as

$$\mathbf{F}^{R_1,R_2} = \mathbf{F}^{R_1} \otimes \mathbf{F}^{R_2} \tag{14}$$

where $\otimes$ denotes tensor product, R_1 and R_2 are the individual fractional orders in two dimensions. For a 2D digital image $\mathbf{P}$, its MRFrFT can be computed as:

$$\mathbf{P}_R = \mathbf{F}^{R_1,R_2}(\mathbf{P}) = \mathbf{F}^{R_1} \cdot \mathbf{P} \cdot \mathbf{F}^{R_2} \tag{15}$$

B. The Main Features and Properties of the MRFrFT

- The proposed MRFrFT is completed by carrying out three steps and each step introduces random parameters which can be used as the private keys in image encryption. Thus, the randomness of the MRFrFT is guaranteed by the random coefficients vector $\mathbf{B}$, the $2(N-K)$ RPOMs, and the logistic map parameters x_0, p and the integer K. Therefore, the proposed MRFrFT has total $2(N-K)+4$ private keys.
- If $K=0$, the kernel functions of all channels will be randomized, and the MRFrFT will degrade into (8).
- If $K=N$, the MRFrFT will degrade into random Fourier transform (RFT) proposed in [18].
- Linearity. The MRFrFT is a linear transform,

$$\mathbf{F}^R\{c_1 f(x) + c_2 f(y)\} = c_1 \mathbf{F}^R\{f(x)\} + c_2 \mathbf{F}^R\{f(y)\} \tag{16}$$

Proof: From the linearity of the DFrFT and the construction process of the MRFrFT, this property can be proved trivially.

- Parseval. The MRFrFT satisfy the Parseval theorem.

$$\sum_{n=0}^{N-1} |\mathbf{x}(n)|^2 = \sum_{k=0}^{N-1} |\mathbf{X}_R(k)|^2 \tag{17}$$

Proof: Because $\mathrm{DFT}\{B_n^{R_n}\} = \exp[-j(\pi/2)k \cdot \mathrm{Rand}(n)]$ are randomly chosen on the unit circle, and the RPOMs in (7) are pure phases [14], combined the energy conservation property of DFrFT, this property is tenable.

C. Discussion of the Computation Cost of the MRFrFT

When executing the proposed MRFrFT on a computer, the kernel functions $\mathbf{F}^{nb}, n=0,1,\cdots,N-1$ can be pre-computed and stored. Once the transform order or the parameters are changed, we only need to re-compute the coefficients of every channel and the matrix multiplications between kernel functions and the corresponding RPOMs. Therefore, the computation cost of the MRFrFT is greatly reduced comparing with other FrFT expansions. Note that the MRFrFT takes up memory space for reducing the running time. Since the linear summation still takes $O(N^2)$ multiplications, the computation complexity for each transform signal is still $O(N^2)$ just as the discussion in [13].

TABLE I
COMPARISON OF COMPUTATION TIME BETWEEN THE PROPOSED MRFrFT AND FrFT EXPANSIONS

Method	Computation time (s) (128× 128)	Computation time (s) (256× 256)	Computation times (s) (512× 512)
DFrFT	0.41761	4.27308	70.75624
MPDFrFT	0.44934	4.31678	70.42953
RFrFT	1.29342	14.9103	219.9258
RDFrFT	3.52712	42.8361	651.79362
MRFrFT	**0.23718**	**0.79624**	**6.35184**

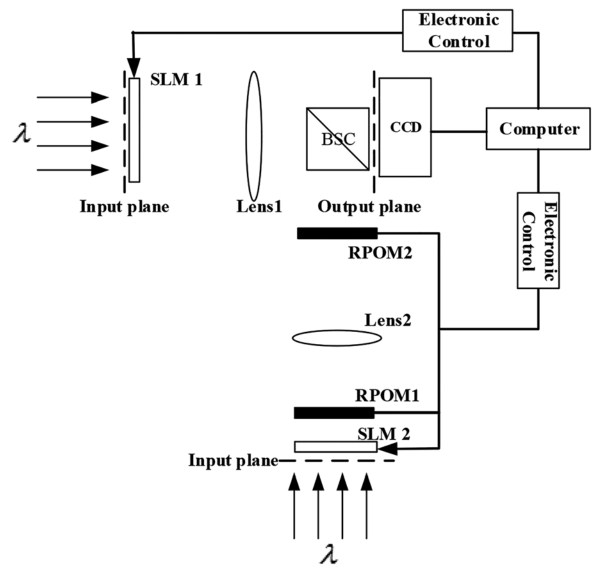

Fig. 2. Optoelectronic implementation of the MRFrFT.

To make a comparison of running time quantitatively between the MRFrFT and other FrFT expansions, we use the 2D image $\mathbf{P}$ with size $N \times N$ to execute the following operators:

$$\mathbf{Q} = \mathbf{L}^a \cdot \mathbf{P} \cdot \mathbf{L}^b \tag{18}$$

where $N = 128, 256, 512$, $\mathbf{L}^a$ and $\mathbf{L}^b$ denote the operators of the FrFT expansions or the MRFrFT with different orders. Table I records the calculating time of all transforms and verifies that the computation cost of the MRFrFT is very much reduced.

D. Optoelectronic Implementation of the MRFrFT

The proposed MRFrFT can be carried out both electronically and optically. Fig. 2 illustrates an optoelectronic hybrid system in double optical paths with iterative mechanism. Lohmman's single lens configuration is used to perform the FrFT [15]. The two spatial light modulators (SLM), which can display complex data, are located at the two input planes and serve to display the iterative results $\mathbf{Fr}_n(x,y)$ and $\mathbf{Rand}_{d(m)}(x,y)$. The RPOM1 and RPOM2 controlled by a computer serve to display $\mathbf{P}^1_{d(m)}$ and $\mathbf{P}^2_{d(m)}$. The beam splitter cube (BSC) is used to split or combine laser beam. At the output plane, the resultant function can be recorded by a holographic scheme with a CCD and then fed to a computer. After post processing in the computer with other parameters, exact information on the amplitude and phase is retrieved and displayed in the SLM for the next iteration. The decryption process can be implemented on a computer.

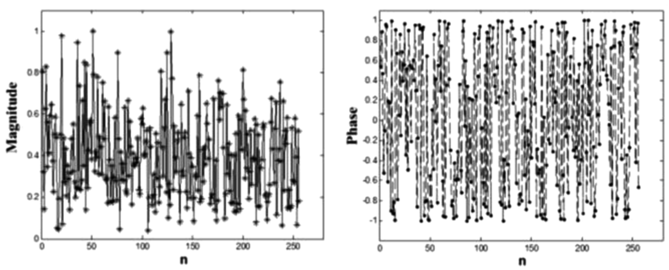

Fig. 3. The MRFrFT of a 1D rectangular function. (a) The output magnitude, (b) The output phase.

IV. Numerical Simulations of The MRFrFT

In our numerical operations, we used a computer with Intel-i5, 3.2 GHz CPU and 8G memory under Windows 7 system. The simulation is implemented in the environment with MATLAB R2012b. We use the following parameters to compute the MRFrFT operator defined in (12). For simplicity, the random weighting coefficients defined in (5) is also produced based on the logistic map function (9) with parameters $x_{01} = 0.3412$, $p_1 = 3.9537$. $\mathbf{Rand}$ defined in (10) is computed with the parameters $x_{02} = 0.2135$, $p_2 = 3.9898$, and $K = 249$. That is, 7 channels are chosen to be randomized with 7 couple PROMs that are produced from a random number generator in MATLAB. For all of the numerical simulations in this paper, we use the same parameters which can be viewed as the private keys in image decryption process.

We use a rectangle function given as follows to simulate the 1D numerical results.

$$x(n) = \begin{cases} 1, & \text{if } 100 < n \leq 155 \\ 0, & \text{otherwise} \end{cases} \tag{19}$$

Here we have taken the number of sample points equal to 256. By applying the process defined in (13), the MRFrFT of 1D rectangle function is calculated and the numerical results are depicted in Fig 3. It demonstrates an important feature of the proposed MRFrFT that the magnitude and phase of its output are both random.

The proposed MRFrFT can be directly used in image encryption by executing (15). The security is guaranteed by large key space composed by the random coefficients vector $\mathbf{B}$, the logistic map parameters x_0, p and K, and the $2(N-K)$ RPOMs. The decryption schematic is the inverse process of the image encryption. Fig. 4 illustrates the image encryption and decryption results by using a gray image "lena" with 256×256 pixels. It can be seen that slight variations of the keys will cause strong damage to the decryption image and cannot identify them visually.

The security is also analyzed quantitatively by calculating the mean square error (MSE) defined as

$$\mathrm{MSE} = \left(\sum_{m=1}^{M} \sum_{n=1}^{N} \left|\left|D\left(m,n\right)\right| - \left|O\left(m,n\right)\right|\right|^2\right) / (M \times N) \tag{20}$$

where $M \times N$ are the size of the image, $D(m,n)$ and $O(m,n)$ are the pixel values of the decrypted and the original image, respectively.

Table II shows the MSE with incorrect keys and verify that the proposed method is sensitive to all of the $2(N-K)+4$ private keys.Fig. 5 compares the security between RDFrFT, RFrFT, and MRFrFT, all of which can be directly used in image encryption, from the results of the MSE. The x-axis δ represents the deviation distance (in the interval $[-0.0008, 0.0008]$ with step size

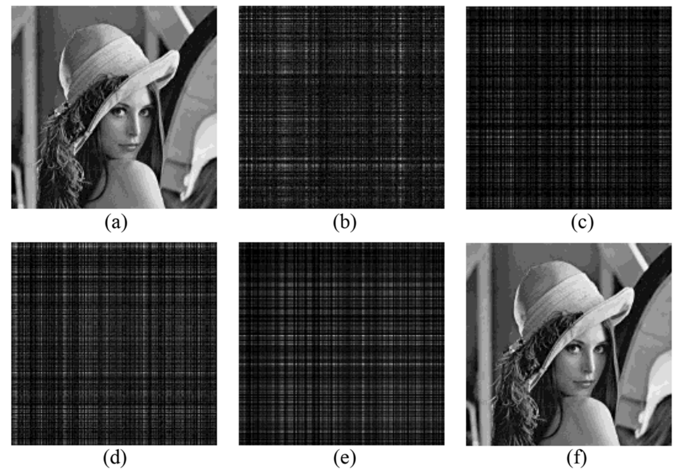

Fig. 4. Results of image encryption and decryption with the MRFrFT. (a) Original image, (b) encrypted image, (c) decrypted image with incorrect weighting coefficients $p_1 = 0.9562$, (d) decrypted image with incorrect logistic map parameters $x_{02} = 0.2112$, (e) decrypted image with a couple incorrect RPOMs in the first chosen channel, (f) decrypted image with correct keys.

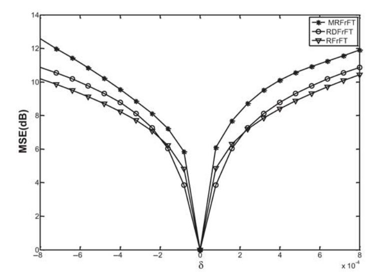

Fig. 5. Comparison of the MSE between the proposed MRFrFT and the FrFT random expansions.

TABLE II
The MSE of The Proposed MRFrFT With Incorrect Parameters

Incorrect Parameters	Coefficients	x_0	p	K			
MSE	3.51×10^{10}	1.21×10^{8}	1.48×10^{8}	1.12×10^{9}			
Incorrect Parameters	The Number of Channels with Incorrect RPOMs						
	1	2	3	4	5	6	7
MSE	2.87×10^{7}	4.97×10^{6}	1.41×10^{6}	5.67×10^{6}	4.97×10^{6}	7.84×10^{6}	1.32×10^{6}

0.00008) to the correct transform order parameters. Fig. 5 indicates that the MRFrFT is more sensitive to the variations of the transform order, which means higher security level than other FrFT random expansions. The above simulation results demonstrate that the proposed encryption scheme has high security due to the large key space and the sensitivity to the private keys.

V. Conclusion

In this letter, we propose an efficient MRFrFT with random weighting coefficients and partial channel transform kernel functions. It can be carried out both electronically and optically. This proposed transform is also able to be used in color image encryption and multi-image encryption with high security and efficiency.

REFERENCES

[1] H. M. Ozaktas, Z. Zalevsky, and M. A. Kutay, *The Fractional Fourier Transform with Applications in Optics and Signal Processing*. New York, NY, USA: Wiley, 2000.

[2] R. Torres and E. Torres, "Fractional Fourier analysis of random signals and the notion of α-stationarity of the wigner-ville distribution," *IEEE Trans. Signal Process.*, vol. 61, no. 6, pp. 1555–1560, Mar. 2013.

[3] Z. J. Liu, M. A. Ahmad, and S. T. Liu, "A discrete fractional angular transform," *Opt. Commun.*, vol. 281, pp. 1424–1429, Jul. 2008.

[4] X. L. Chen, J. Guan, Z. H. Bao, and Y. He, "Detection and extraction of target with micromotion in spiky sea clutter via short-time fractional Fourier transform," *IEEE Trans. Geosci. Remote Sens.*, vol. 52, no. 2, pp. 1002–1018, Feb. 2014.

[5] L. S. Sui, K. K. Duan, J. L. Liang, and X. H. Hei, "Asymmetric double-image encryption based on cascaded discrete fractional random transform and logistic maps," *Opt. Exp.*, vol. 22, no. 9, pp. 10605–10621, May 2014.

[6] M. G. Shan, J. Chang, Z. Zhong, and B. G. Hao, "Double image encryption based on discrete multiple-parameter fractional Fourier transform and chaotic maps," *Opt. Commun.*, vol. 285, no. 21, pp. 4227–4234, Jul. 2012.

[7] F. Zhang, Y. Hu, R. Tao, and Y. Wang, "New fractional matrix with its applications in image encryption," *Opt. Laser Technol.*, vol. 64, pp. 82–93, Jun. 2014.

[8] L. S. Sui, M. T. Xin, A. L. Tian, and H. Y. Jin, "Single-channel color image encryption using phase retrieve algorithm in fractional Fourier domain," *Opt. Lasers Eng.*, vol. 51, no. 12, pp. 1297–1309, Jun. 2013.

[9] S. C. Pei and M. H. Yeh, "Improved discrete fractional Fourier transform," *Opt. Lett.*, vol. 22, no. 14, pp. 1047–1049, Jul. 1997.

[10] S. C. Pei and W. L. Hsue, "The multiple-parameter discrete fractional Fourier transform," *IEEE Signal Process. Lett.*, vol. 13, no. 6, pp. 329–332, Jun. 2006.

[11] Z. J. Liu, H. F. Zhao, and S. T. Liu, "A discrete fractional random transform," *Opt. Commun.*, vol. 255, no. 4, pp. 357–365, Jun. 2005.

[12] S. C. Pei and W. L. Hsue, "Random discrete fractional Fourier transform," *IEEE Signal Process. Lett.*, vol. 16, no. 12, pp. 1015–1018, Dec. 2009.

[13] M. H. Yeh and S. C. Pei, "A method for the discrete fractional Fourier transform computation," *IEEE Trans. Signal Process.*, vol. 51, no. 3, pp. 889–891, Mar. 2003.

[14] Z. J. Liu and S. T. Liu, "Random fractional Fourier transform," *Opt. Lett.*, vol. 32, no. 15, pp. 2088–2090, Aug. 2007.

[15] A. W. Lohmann, "Image rotation, wigner rotation, and the fractional Fourier transform," *J. Opt. Soc. Am. A*, vol. 10, no. 10, pp. 2181–2186, Oct. 1993.

[16] L. B. Almeida, "The fractional Fourier transform and time-frequency representations," *IEEE Trans. Signal Process.*, vol. 42, no. 11, pp. 3084–3091, Nov. 1994.

[17] H. M. Ozaktas, B. Barshan, D. Mendlovic, and L. Onural, "Convolution, filtering, and multiplexing in fractional Fourier domains and their relation to chirp and wavelet transforms," *J. Opt. Soc. Amer. A*, vol. 11, no. 2, pp. 547–559, Feb. 1994.

[18] Z. J. Liu and S. T. Liu, "Randomization of the Fourier transform," *Opt. Lett.*, vol. 32, no. 5, pp. 478–480, Mar. 2007.